Experimental report

13/09/2024

Proposal: 9-12-698 **Council:** 4/2023

Title: Elucidating the adsorption mechanism of a molecular water pollutant in the organic shell of nanoparticulate water cleaning agents

Research area: Materials

This proposal is a new proposal

Main proposer: Lukas MUELLER

Experimental team: Lukas MUELLER
Wenke MUELLER

Local contacts: Ralf SCHWEINS

Samples: SPIONs (Fe2O3) decorated with PAC3Imida (C7H14BrN2O3P) and PAC18 (C18H39O3P) + 17-beta estradiol (C18H24O2)

Instrument	Requested days	Allocated days	From	To
D22	2	1	06/09/2023	07/09/2023
D33	0	0		

Abstract:

General access to clean water is a major global challenge. Anthropogenic molecular pollutants, like herbicides or hormones are present in our surface waters due to careless disposal and insufficient remediation. Therefore, it exists a strong demand in affordable and efficient removal of such contaminants from water. We work on superparamagnetic iron oxide nanoparticles (SPIONs) that are decorated with self-assembled monolayers (SAMs) composed of permanently binding phosphonic acid derivates to address certain interaction motifs of surrogate pollutants (e.g. hormone 17-beta estradiol). Such particles attract the pollutants and can be easily remediated from water by an external magnetic field. We envision sorbent systems that are not only thermodynamically attractive for the pollutants of choice, but also present suitably-sized nano-cavities in the binary SAM. Understanding how the pollutant actually adsorbs "in or on" the cavity-enriched SAM is an experimentally challenging task, for which SANS with contrast variation is one of the few available techniques. Elucidating the adsorption mechanism would benefit the improvement of design for such water cleaning agents.

Experimental Report - Proposal Number 9-12-698

Aim

It was aimed to investigate the morphology of a binary self-assembled monolayer (SAM) on superparamagnetic iron oxide nanoparticles (SPIONs) and changes to that monolayer upon adsorption of 17-β Estradiol (E2) at low concentrations. Ideally, the presented investigation would permit the localization of E2 in the SAM.

Scientific Background

Anthropogenic molecular pollutants, like herbicides or hormones are present in our ground water and find their way into drinking water due to careless disposal and insufficient remediation. Therefore, it exists a big demand in affordable and efficient removal of such contaminants from water. Basing on previous work,[1–4] we develop surface functionalized SPIONs that address certain interaction motifs of selected surrogate pollutants (e.g. 17-β estradiol, E2). Such particles attract the pollutants and can be easily remediated from water by an external magnetic field. The binary SAM designed for E2 consists of permanently binding phosphonic acid derivates, 1-methyl-3-(propylphosphonic acid) imidazolium bromide (PAC_3Imi+) and n-octadecylphosponic acid (PAC_{18}). Those molecules self-assemble in a two-step process on maghemite SPIONs (PAC_3Imi+/PAC_{18}@SPIONs) with our aim to present hydrophobic cavities with positively charged motifs, in which the E2 molecules may thermodynamically and sterically fit. Despite promising experimental results in the removal of E2 from water, the exact adsorption mechanism on the nanoparticle surface remains unclear.

Experimental

For the samples (PAC_3Imi+/PAC_{18}@SPIONs with adsorbed E2 and without) presented in this report, 1±0.03 mg of coated SPIONs was predispersed in 50 µL of acetonitrile under sonication. For the sample without E2, 7 mL of degassed D_2O was added followed by 10 min vortex mixing at 500 rpm and subsequent transfer to a quartz cuvette. Respectively, 7 mL of degassed D_2O containing 1 µM of E2 and 1 vol% of acetonitrile (standard procedure) were added to the other sample. After 10 min of vortex mixing at 500 rpm an aliquot was transferred to a quartz cuvette too. Experiments were performed on the small angle neutron scattering (SANS)-instrument D22. A circular neutron beam with a diameter of 12 mm was used. Cuvettes were placed in a tumbling rack and continuously rotated during the measurement to avoid sedimentation. For the successful measurements shown in this report, quartz cuvettes with a path length of 5 mm were used, because samples were prepared in D_2O. The D22 instrument possesses two detectors: The front detector, which was at a fixed distance of 1.4 m to the sample and a rear detector. Most measurements were carried out at a sample-to-rear detector distance of 4 m (collimation 4 m) at a neutron wavelength of 6 Å to cover a q-range of 0.014 $Å^{-1}$ to 0.61 $Å^{-1}$. Neutrons were detected with two ^3He detectors (multi-tube detector consisting of vertically aligned Reuter-Stokes tubes, with 128 tubes for the rear and 96 tubes for the front detector, all with a diameter of 8 mm and a pixel size of 8 mm x 8 mm). Detector images were corrected to the transmission of the direct beam, scaled to absolute intensity and azimuthally averaged using the GRASP software.[5] Empty cell and solvent scattering were subtracted from the scattering curves.[6] SANS curves were fitted (DREAM algorithm, 10^6 samples for each initial fit) using the SasView 5.0.6 software package.

Results

It was intended to obtain information on the binary SAM on the SPIONs as well as changes upon adsorption of E2. Due to the low concentration of SPIONs and E2 in the sample, only a weak scattering signal was observed, rendering the high-flux instrument D22 ideally suited for the presented experiment. Data interpretation is furthermore hampered by the propensity of the hydrophobic SPIONs to aggregate, which needs to be considered during fitting. In the presented case, a q^{-4} dependency of the low-q scattering intensity was used to account for these large aggregates (Porod law)[6] that was complemented with a form factor $P_{model}(q)$ to represent the contribution of individual SPIONs:

$$I(q) = A \cdot q^{-4} + B \cdot P_{model}(q) + bkg \quad (1)$$

In Equation (1), q is the value of the scattering vector, $I(q)$ the intensity, A and B are scaling factors and bkg is the incoherent background. As the investigated PAC_3Imi+/PAC_{18}@SPIONs are approximately spherical, they were described using either the form factor of a core-shell sphere with linearly varied scattering length density (SLD) in the shell region ($P_{\text{core-shell}}$) or a core-shell-shell sphere with linearly varied SLD in both shells ($P_{\text{core-shell-shell}}$). The SLD profiles as well as the relevant parameters (fitted or fixed) are illustrated in Figure 1.

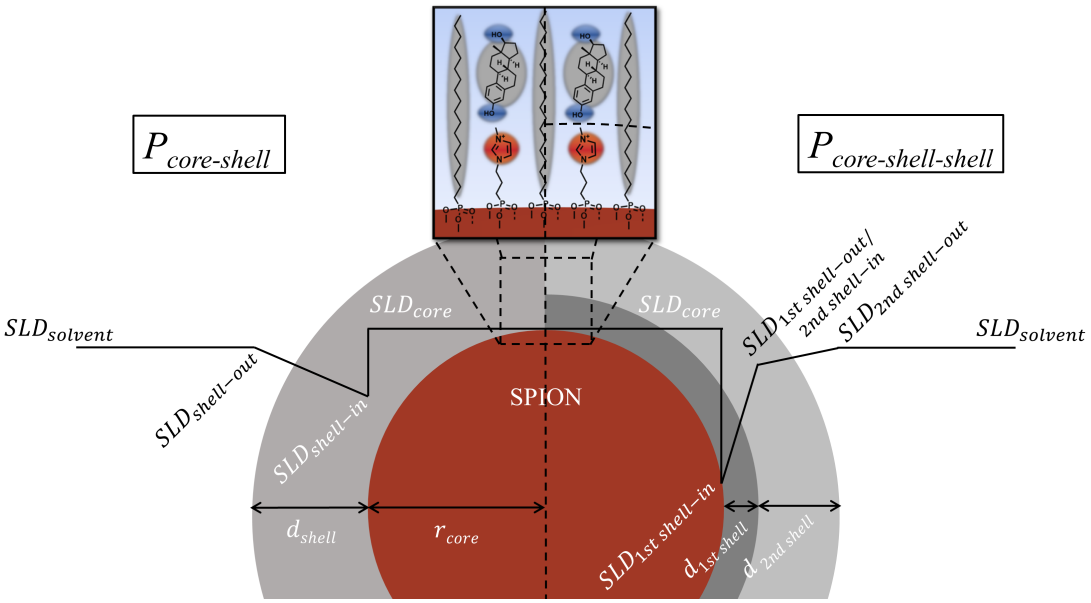

Figure 1: Schematic representation of a PAC_3Imi+/PAC_{18}@SPION with illustrated SLD profiles applied in the form factor models $P_{core\text{-}shell}$ (left) and $P_{core\text{-}shell\text{-}shell}$ (right).

Due to the low intensity gathered from the low concentrated samples, information from other techniques and simulations was incorporated into the models resulting in the fits displayed in Figure 2. All fixed and fitted parameters as well as their set limits basing on physical reason are given in Table 1. r_{core} was estimated from gas adsorption experiments, limits/fixed values of d_{shell}, $d_{1st\ shell}$ and $d_{2nd\ shell}$ were estimated via the potential molecule lengths with Chem3D, $SLD_{core/solvent}$ were calculated and the limits/fixed values of $SLD_{shell\text{-}in/out}$ were estimated from the ratio of PAC_3Imi+/PAC_{18} determined by infrared spectroscopy corrected by the content of D_2O calculated from molecular dynamics simulations. To improve fit quality, $SLD_{shell\text{-}in}$ and $SLD_{2nd\ shell\text{-}in}$ needed to be fitted for PAC_3Imi+/PAC_{18}@SPIONs (fixed for the sample with E2).

Judging from the respective χ^2_{red}, PAC_3Imi+/PAC_{18}@SPIONs is better respresented by $P_{\text{core-shell}}$ while PAC_3Imi+/PAC_{18}@SPIONs + E2 is equally good represented by both models. The obtained d_{shell} for the sample without E2 indicates a collapsed state for PAC_{18} molecules while d_{shell} as well as $d_{2nd\ shell}$ for the sample with E2 point to an erection upon E2 adsorption (as there are only few E2 molecules per SPION, simple adsorption on top of SAM is unlikely). These results support the existing hypothesis that the alkyl chain of PAC_{18} does not extend into the surrounding medium in the absence of E2 due to hydrophobic effects. Upon addition of E2, however, the case displayed in the inset of Figure 1 seems more likely, which leads to PAC_{18} being more extended, resulting into the observation of a thicker SAM.

(1) M. Sarcletti, D. Vivod, T. Luchs, T. Rejek, L. Portilla, L. Müller, H. Dietrich, A. Hirsch, D. Zahn and M. Halik, *Adv. Funct. Mater.*, **2019**, 29, 1805742.
(2) M. Sarcletti, H. Park, J. Wirth, S. Englisch, A. Eigen, D. Drobek, D. Vivod, B. Friedrich, R. Tietze, C. Alexiou, D. Zahn, B. Apeleo Zubiri, E. Spiecker and M. Halik, *Mater. Today*, **2021**, 48, 38–46.
(3) A. Eigen, L. M. S. Stiegler, S. Gradl, V. Schneider, V. Wedler, H. Gaß, L. Müller, M. Sarcletti, M. R. Heinrich, A. Hirsch and M. Halik, *Adv. Mater. Interfaces*, **2022**, 9, 2201471.
(4) A. Eigen, V. Schmidt, M. Sarcletti, S. Freygang, A. Hartmann-Bausewein, V. Schneider, A. Zehetmeier, V. Mauritz, L. Müller, H. Gaß, L. Rockmann, R. W. Crisp and M. Halik, *Nano Select*, **2024**, 5, 2300130.
(5) C. D. Dewhurst, *J. Appl. Crystallogr.*, **2023**, 56, 1595–1609.
(6) P. Lindner and T. Zemb, *Neutrons, X-rays, and light : scattering methods applied to soft condensed matter*, Elsevier, 1st edn., **2002**.

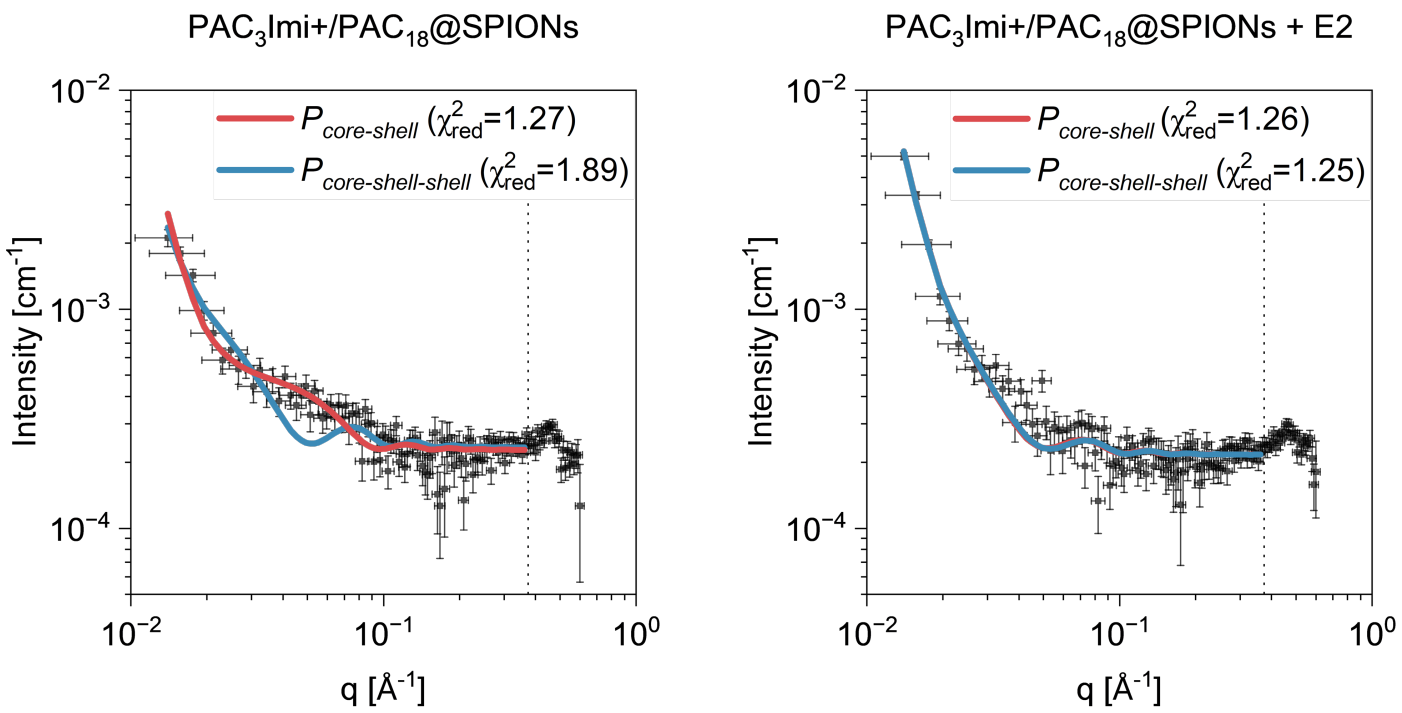

Figure 2: Recorded SANS data as well as fits of PAC_3Imi+/PAC_{18}@SPIONs without (left) and with adsorbed E2 (right). The core-shell model represents the data of the SPIONs without E2 much better, while the SPIONs with adsorbed E2 are represented well by both models. Data with bigger q than 0.374 $Å^{-1}$ (dotted lines) was not regarded as being attributed with large measurement artefacts.

Table 1: Models and parameters (fixed and fitted) for fit graphs in Figure 1.

Models for *I(q)*, parameters and limits	**PAC_3Imi+/PAC_{18}@SPIONs**	**PAC_3Imi+/PAC_{18}@SPIONs + E2**
$A \cdot q^{-4} + B \cdot P_{core-shell} + bkg$	$\chi^2_{red} = 1.27$	$\chi^2_{red} = 1.26$
$A\ [-\infty; \infty]$	$(3.36 \pm 0.27) \cdot 10^{-11}$	$(6.90 \pm 0.28) \cdot 10^{-11}$
$B\ [-\infty; \infty]$	$(3.79 \pm 0.74) \cdot 10^{-4}$	$(5.85 \pm 0.81) \cdot 10^{-6}$
$r_{core}\ (fixed)$	53.65 Å	53.65 Å
$SLD_{core}\ (fixed)$	$6.66 \cdot 10^{-6} Å^{-2}$	$6.66 \cdot 10^{-6} Å^{-2}$
$SLD_{shell-in}\ [2.87; 6.39] \cdot 10^{-6} Å^{-2}$	$(5.70 \pm 0.23) \cdot 10^{-6} Å^{-2}$	$2.87 \cdot 10^{-6} Å^{-2}\ (fixed)$
$SLD_{shell-out}\ (fixed)$	$6.39 \cdot 10^{-6} Å^{-2}$	$6.39 \cdot 10^{-6} Å^{-2}$
$SLD_{solvent}\ (fixed)$	$6.39 \cdot 10^{-6} Å^{-2}$	$6.39 \cdot 10^{-6} Å^{-2}$
$d_{shell}\ [7; 32.6]$ Å	7.03 ± 4.45 Å	17.84 ± 5.57 Å
$bkg\ [-\infty; \infty]$	$(2.25 \pm 0.04) \cdot 10^{-4}$	$(2.14 \pm 0.03) \cdot 10^{-4}$
$A \cdot q^{-4} + B \cdot P_{core-shell-shell} + bkg$	$\chi^2_{red} = 1.89$	$\chi^2_{red} = 1.25$
$A\ [-\infty; \infty]$	$(2.11 \pm 0.28) \cdot 10^{-11}$	$(6.92 \pm 0.27) \cdot 10^{-11}$
$B\ [-\infty; \infty]$	$(1.65 \pm 0.67) \cdot 10^{-5}$	$(7.46 \pm 1.02) \cdot 10^{-6}$
$r_{core}\ (fixed)$	53.65 Å	53.65 Å
$SLD_{core}\ (fixed)$	$6.66 \cdot 10^{-6} Å^{-2}$	$6.66 \cdot 10^{-6} Å^{-2}$
$SLD_{1st\ shell-in}\ (fixed)$	$0.24 \cdot 10^{-6} Å^{-2}$	$0.24 \cdot 10^{-6} Å^{-2}$
$SLD_{1st\ shell-out}\ (fixed)$	$5.49 \cdot 10^{-6} Å^{-2}$	$5.49 \cdot 10^{-6} Å^{-2}$
$d_{1st\ shell}\ (fixed)$	7 Å	7 Å
$SLD_{2nd\ shell-in}\ [5.49; 6.39] \cdot 10^{-6} Å^{-2}$	$(5.92 \pm 0.27) \cdot 10^{-6} Å^{-2}$	$5.49 \cdot 10^{-6} Å^{-2}\ (fixed)$
$SLD_{2nd\ shell-out}\ (fixed)$	$6.39 \cdot 10^{-6} Å^{-2}$	$6.39 \cdot 10^{-6} Å^{-2}$
$SLD_{solvent}\ (fixed)$	$6.39 \cdot 10^{-6} Å^{-2}$	$6.39 \cdot 10^{-6} Å^{-2}$
$d_{2nd\ shell}\ [0; 25.6]$ Å	14.58 ± 7.33 Å	12.61 ± 6.93 Å
$bkg\ [-\infty; \infty]$	$(2.23 \pm 0.04) \cdot 10^{-4}$	$(2.13 \pm 0.03) \cdot 10^{-4}$